Evidence for mantle heterogeneities in the westernmost Mediterranean from a statistical approach to volcanic petrology

Massimiliano Melchiorre [1,*], Jaume Vergés [1], Manel Fernàndez [1], Massimo Coltorti [2], Montserrat Torne [1], and Emilio Casciello [1].

[1] Group of Dynamics of the Lithosphere, Institute of Earth Sciences Jaume Almera ICTJA – CSIC, Lluís Solé i Sabarís s/n, 08028 Barcelona, Spain

[2] Department of Physics and Earth Sciences, Ferrara University, via Saragat 1, 44123 Ferrara, Italy.

* Corresponding author.

E-mail address: mmelchiorre@ictja.csic.es (M. Melchiorre)

Abstract

The geological evolution of the Westernmost Mediterranean is characterised by widespread volcanic activity, with subductive (orogenic) or intraplate (anorogenic) geochemical imprints. The geochemical features of major and trace elements, and the isotopic ratios of 283 orogenic and 310 anorogenic samples of the Western and Central Mediterranean were merged in a unique database that was processed by using a statistical approach. The factor analysis, performed by using the Principal Component Analysis (PCA) method, reduced the original 36 geochemical parameters that were expressed as oxides, elements or isotopic ratios to seven factors, accounting for ~84% of variance. Combining these factors in binary diagrams allows separating the anorogenic and orogenic fields. Anorogenic samples usually fall into a narrow compositional range, while orogenic rocks are characterised by a greater variability and by alignment along different trends. These different trends account for large heterogeneities of the lithospheric mantle in the Mediterranean area due to extensive recycling of geochemically different lithologies, at least since Palaeozoic times, thus supporting the existence of different mantle reservoirs as being responsible for the Mediterranean volcanism. We find that the double subduction polarity model, that was recently proposed for the Westernmost Mediterranean, is compatible with the volcanic petrology of the last 30 My.

Keywords

Factor analysis, Geochemical database, Major elements, Trace elements, Isotopic ratios, Geodynamic evolution, Orogenic volcanism, Anorogenic volcanism.

1. Introduction

The Central and Western Mediterranean encompasses the region between the Calabrian and the Gibraltar arcs, including a series of Neogene marine sedimentary basins (e.g., Alboran, Valencia Trough, Algerian, Liguro-Provençal, and Tyrrhenian), the surrounding Alpine belts (e.g., Betics, Catalan Coastal Ranges, Alps, Apennines, Rif-Tell-Atlas), the Balearic Promontory, and the Corsica-Sardinia block. The whole region forms part of the western Africa-Eurasia plate boundary, where a far-field compressive stress regime was coeval with regional extension, with active and recent subduction processes, and it is characterised by Neogene to recent volcanic activity.

The Central and Western Mediterranean has been widely investigated with the following aims: 1) reconstruct the plate kinematics (e.g., Rabinowitz and LaBrecque, 1979; Dewey et al., 1989; Van der Voo, 1993; Rosenbaum et al., 2002b; Vergés and Fernàndez, 2012; Carminati et al., 2012; Turco et al., 2012; Casciello et al., 2015); 2) emphasise the seismic images in order to propose snapshots of the actual lithospheric domains beneath Europe and the Mediterranean (e.g., Gutscher et al., 2002; Piromallo and Morelli, 2003; Spakman and Wortel, 2004; Wortel et al., 2009; Giacomuzzi et al., 2012; Bezada et al., 2013; Palomeras et al., 2014; Thurner et al., 2014; Chiarabba et al., 2014); and 3) describe the volcanic activity that affected several areas from Spain to northern Italy and from northern Africa to Central Europe since the Oligocene (El Azzouzi et al., 1999; Coulon et al., 2002; Beccaluva et al., 2004, 2013; Harangi et al., 2006; Lustrino and Wilson, 2007; Lustrino et al., 2011; Carminati et al., 2012; El Azzouzi et al., 2014). The volcanic activity in Central and Western Mediterranean can be broadly divided into two main types (Fig. 1) on the basis of their tectonic and geochemical features (see Lustrino and Wilson, 2007 and Lustrino et al., 2011 for

67 reviews). Orogenic or subduction-related volcanism usually refers to those volcanic
68 rocks that are generated in a continent-continent collision or associated with the
69 subduction of oceanic lithosphere (e.g., Carminati and Doglioni, 2004) and comprises
70 arc tholeiitic, calc-alkaline, High Potassium (HK) calc-alkaline, shoshonitic and
71 ultrapotassic products. In these areas, anorogenic or intraplate volcanism is associated
72 with a post-collisional environment and includes alkaline rocks with sodic affinity.
73 Combining this information, several and sometimes competing geodynamic models
74 were put forward to explain the Tertiary evolution of the Western Mediterranean
75 (Doblas et al., 2007).

76 Tomography models resulted in a consensus on the extent, shape and dip of the present-
77 day subducting slabs in the region. However, discrepancies arise on the subduction
78 initiation relative to the extent of the subduction front, its orientation and dip. Some
79 authors propose an initial N-NW dipping subduction front that extends from the Alps to
80 the present-day Gibraltar Arc (e.g., Faccenna et al., 2004; Schettino and Turco, 2006;
81 Carminati et al., 2012). Some other authors propose restrictions on the initial N-NW
82 dipping subduction zone from the Alps to the southwest termination of the present-day
83 Balearic Promontory (e.g., Rosenbaum and Lister, 2004; Spakman and Wortel, 2004;
84 van Hinsbergen et al., 2014). A third model proposes a lateral change in the initial
85 subduction polarity from S-SE along the north Moroccan margin to N-NW along the
86 Balearic Promontory until the Alps (Vergés and Fernàndez, 2012; Casciello et al.,
87 2015).

88 The incorporation of volcanism in these models is uneven. Duggen et al. (2004, 2005)
89 explain the geochemical features of the westernmost Mediterranean volcanism as due to
90 delamination in a context of a westward roll-back phase. Booth-Rea et al. (2007) use the
91 volcanism to support a model in which an E-dipping subduction beneath the Alboran

92 and Algero-Balearic basins was active until the late Miocene, when it stopped, probably
93 due to the complete consumption of the oceanic crust. The Si-K rich volcanism is
94 interpreted as due to anatexis resulting from the direct contact of the asthenosphere with
95 the base of the crust, driven by the delamination of the lithospheric mantle (Bird, 1979).
96 Wilson and Bianchini (1999) provide clues for the origin of the most primitive mafic
97 igneous rocks that can be considered as the best indicator for the initial geodynamic
98 setting. Harangi et al. (2006) deal with the subduction-related volcanic rocks and their
99 relation with competing geodynamic models that are proposed for the evolution of the
100 Central and Western Mediterranean. Finally, Lustrino and different co-workers
101 (Lustrino and Wilson, 2007; Lustrino et al., 2011; Lustrino, 2011) present an overview
102 of the two main geochemically different rocks, erupted in the Mediterranean
103 (anorogenic and orogenic), with an aim of providing a general model for the
104 petrogenesis of the intraplate affinity suite and a possible relationship between the
105 tectonic evolution and the geochemistry of the subduction-related rocks.

106 The huge amount of available information on the geochemistry of the volcanic products
107 in the Western and Central Mediterranean makes its incorporation into the proposed
108 geodynamic models difficult, mainly due to their extreme chemical heterogeneity. A
109 way to manage large numbers of variables with no obvious relationships among them is
110 the use of the factor analysis technique. Although this technique is being used widely in
111 the social and life sciences and is becoming a common method in earth science, it is not
112 yet used in volcanic geochemistry. In this paper, we present the results obtained by
113 applying, for the first time, a factor analysis (using the principal component method) to
114 a large database composed of Mediterranean orogenic (Lustrino et al., 2011) and
115 anorogenic (Lustrino and Wilson, 2007) volcanic rocks. Factor analysis is here used to
116 remove redundant variables and to replace the entire geochemical data file by a smaller

number of variables in order to support previous geochemical interpretations and to ascertain the utility of the method.

Our main aims are: 1) to verify whether a factor analyses technique can be applied to geochemical issues; 2) to highlight the differences in terms of geochemical composition of the intraplate affinity and subduction-related volcanic rocks of the Western and Central Mediterranean and their temporal evolution; and 3) to constrain the origin of the mantle heterogeneities representing the source of the volcanism. Furthermore, we analyse the compatibility between the geochemical signature of the volcanism in the Westernmost Mediterranean and a recently proposed geodynamic model based on a lateral change of the subduction polarity (Vergés and Fernàndez, 2012; Casciello et al., 2015).

2. Cenozoic tectonic evolution of the Central and Western Mediterranean

The Central and Western Mediterranean has undergone a complex geodynamic evolution since the early Cretaceous, and with processes that are still active. This complex history is recorded in the Alpine orogeny (Dal Piaz et al., 2003), in the numerous areas where magmatism and orogenesis occurred (Araña et al., 1983; Cebriá and López-Ruiz, 1995; Harangi et al., 2006; Lustrino and Wilson, 2007; Lustrino et al., 2011; Beccaluva et al., 2011, 2013), and in the formation of several back-arc basins that opened due to the roll-back of lithospheric slabs with various retreat directions (e.g., Carminati et al., 2012). These basins (Fig. 1) are the Liguro-Provençal and the Tyrrhenian basins (Van der Voo, 1993; Faccenna et al., 1997; Doglioni et al., 2004), the Valencia Trough and the Algerian Basin (Martí et al., 1992; Torne, 1996; Vergés and

141 Sàbat, 1999; Ayala et al., 2003; Roca et al., 2004; Carballo et al., 2015), and the
142 Alboran Basin (Comas et al., 1992, 1999; García-Dueñas et al., 1992; Torne et al.,
143 2000; Frizon de Lamotte et al., 2004; Soto et al., 2008). The overall tectonic framework
144 in which this evolution occurred is characterised by the convergence between the
145 African and Eurasian plates that was caused by the opening of the southern Atlantic
146 Ocean since the Early Cretaceous. From these times on, Africa moved slowly toward
147 Eurasia with a NE-directed counter-clockwise rotation (Dewey et al., 1989; Mazzoli and
148 Helman, 1994; Rosenbaum et al., 2002a), shifting to a NNW direction at about 40 Ma
149 (Rosenbaum et al., 2002a; 2002b), and finally to a N-S direction (Devoti et al., 2008).

150 It is widely accepted that the evolution of the Central Mediterranean is linked to the
151 roll-back of the Tethyan oceanic lithosphere, that had remained landlocked since the
152 Oligocene. However, despite the consensus among mantle tomography models that
153 image a subducted and partly torn slab beneath the Betic-Rif orogen (e.g., Spakman and
154 Wortel, 2004; Díaz et al., 2012; Miller et al., 2013; Bonnin et al., 2014; Thurner et al.,
155 2014; Fichtner and Villaseñor, 2015), the debate focuses on how to trace backwards the
156 evolution of these subductions to their initial configuration.

157 The earliest tectonic reconstructions considered the Central and Western Mediterranean
158 basins and surrounding chains as resulting from extensional stresses that dismantled the
159 western Alpine belt. This orogenic dismembering produced the radial dispersion of its
160 high pressure–low temperature (HP-LT) ‘collisional’ metamorphic rocks to form the
161 Calabria-Peloritani, Kabilyes and Alboran terranes (Alvarez et al., 1974; Boccaletti and
162 Guazzone, 1974; Alvarez and Shimabukuro, 2009). As argued in Casciello et al. (2015),
163 this initial interpretation had a strong influence on later reconstructions that, in the case
164 of the Westernmost Mediterranean, can be grouped into three different hypotheses:

1) The original Alpine belt formed a continuous chain from the present-day Alps to the Gibraltar area and was related to a NW-directed subduction, at least since the middle Eocene, incorporating the HP-LT metamorphic domains of the future Betic-Rif Internal Zone (Alboran Domain), the Kabylies blocks, and the Calabria-Peloritani units. The further retreat and slab roll-back towards the SE caused the dispersal of the metamorphic units to follow a radial pattern. The Calabria-Peloritani units moved ESE together with the Sardinia-Corsica block during the opening of the Liguro-Provençal Basin, whereas the Kabylies shifted southwards during the opening of the Algerian Basin (e.g., Jolivet and Faccenna, 2000; Faccenna et al., 2004; Faccena et al., 2014). These authors introduced the concept of slab tears in the subducting lithosphere to allow for an independent WSW roll-back in the Gibraltar area, with respect to the overall S-directed roll-back of the Algerian slab. The main criticism of this model is that the formation of the Miocene NW-verging Betic orogen and the S- to E-dipping present-day subduction polarity is hardly explained.

2) A second model proposes that the initial N-NW dipping subduction zone extends from the Alps to the south of the present position of the Balearic Promontory (e.g., Lonergan and White, 1997; Rosenbaum and Lister, 2004; Spakman and Wortel, 2004; van Hinsbergen et al., 2014). According to these authors, and in a manner that is similar to the previous model, this orogenic belt was composed of HP-LT metamorphic units that dismembered radially, due to the slab roll-back. The main difference with the previous model is that the segment of the subduction front, associated with the present Balearic block, underwent a clockwise rotation of ~180º which was accommodated by lithospheric tearing along the North African margin. This allowed for over 500 km of westward movement of the Alboran domain and the E-W opening of the Algerian basin (van Hinsbergen et al., 2014).

3) The latest interpretation has been proposed by Vergés and Fernàndez (2012). Based on the position of high-grade metamorphic rocks with respect to the subduction polarity and several other geological and geophysical constraints, these authors suggest that the Betic-Rif Arc originated from the Oligocene-Miocene north-westward and westward roll-back of the southeast-dipping Ligurian Tethys lithosphere subduction below Africa. In this view, the Late Oligocene-Miocene evolution of the Central and Western Mediterranean is linked to two opposite dipping subductions: a northwest-dipping, southeast-retreating subduction related to the migration of the Kabylies units, and a southeast-dipping, northwest-retreating subduction related to the formation of the Betic-Rif orogen.

3. Geochemical data and factor analysis

Two large databases that are available in the body of literature have collected much of the volcanic activity that has been registered in the Mediterranean from the Oligocene to the present-day (Fig. 1). The compilation of the orogenic-related rocks has been published by Harangi et al. (2006) and more recently by Lustrino et al. (2011), while the geochemical data of the anorogenic rocks are gathered by Lustrino and Wilson (2007), and further updated by Lustrino (2011). For comparison, we also considered the Canary Islands dataset that, as expected, shows a monotonous and unambiguous intraplate signature from Oligocene to Recent.

The main limitation of such large datasets is to visualise the wealth of information they contain. In geochemistry, binary or ternary diagrams are used to identify any significant variation in the chemistry of the samples, combining major and trace elements, and isotopic ratios. However, even if elemental ratios are considered, it is highly unlikely to

observe, at the same time, variations of more than six elements. Hence, typically, several diagrams are used to display the chemical data, which often distract the attention of the researcher from his final goal of unravelling the geochemical evolution of a suite of rocks, and to insert them in a coherent geodynamic framework. In this respect, a statistical approach through factor analysis can help, acting as a powerful tool to combine more elements and allowing us to summarise most of the geochemical variations in few binary diagrams.

The orogenic volcanic dataset of Lustrino et al. (2011) is a compilation of more than 7,000 analysed samples, while its anorogenic counterpart accounts for ~7,800 analyses (Lustrino, 2011). These two large databases have been merged and filtered by choosing those samples that are characterised by the most complete geochemical dataset in terms of:

a) Major elements, expressed as oxides of Si, Ti, Al, Fe, Mn, Mg, Ca, Na, K, P.
b) Trace elements, including Large Ion Lithophile Elements (LILE) - Cs, Rb, Ba, Sr and Pb; High Field Strength Elements (HFSE) - Th, U, Nb, Ta, Zr and Hf; and Rare Earth Elements (REE) - La, Ce, Pr, Nd, Sm, Eu, Gd, Tb, Dy, Ho, Er, Tm, Yb, Y and Lu.
c) Isotopic composition, mainly expressed by $^{87}Sr/^{86}Sr$, $^{143}Nd/^{144}Nd$, $^{206}Pb/^{204}Pb$ $^{207}Pb/^{204}Pb$, $^{208}Pb/^{204}Pb$, $^{208}Pb/^{206}Pb$ and $^{207}Pb/^{206}Pb$.

After filtering, a total of 283 orogenic and 310 anorogenic volcanic samples were selected (Fig. 2). This procedure has led us to completely exclude from the dataset the samples from the Algerian and Tunisian districts, and to select only three samples from Sardinia and one sample from Corsica (Sisco). We built a 593 x 43 matrix in which each row represents a sample and each column represents a variable (i.e., a geochemical

element characterising the sample). This matrix was processed in order to obtain standardised values that are expressed as $Z_i = (x_i - x_m)/\sigma$, where x_i is the non-standardised value of variable x, x_m is the mean value of variable x, and σ is the standard deviation of variable x. The standardisation procedure inflates variables whose variance is small, reduces the influence of variables whose variance is large, and removes the influence of different measurement units in the data by making them dimensionless.

Factor analysis is a multivariate statistical method used to represent a large number of variables in the original data by a substantially smaller number of factors. The term factor in geochemistry refers to controlling processes and factor analysis is ideally suited for an easy presentation of the essential information that is preserved in a geochemical dataset with many elements (Reimann et al., 2002). The aim of this statistical analysis is to reduce the dimensionality of the original space, thus allowing for a most comprehensible interpretation by a reduced number of dimensions which are supposed to underlie the old dimensions (Rietveld and Van Hout, 1993).

For this purpose, the matrix has been processed using the Statistical Package for Social Sciences (SPSS) version 17, that allowed a first reduction of the number of variables to describe the 593 samples by reading the value of the communality (comprised between 0 and 1). The communality of a variable is an automatically calculated parameter, based on the sum of the loadings of this variable on all of the extracted factors, which reflects the percentage of variance in a given variable that is jointly encompassing all of the factors (interpreted as the reliability of the indicator). Those variables with communality lower than 0.6 were considered meaningless and were disregarded. The matrix was reprocessed until all variables had communality greater than 0.6, thus excluding MnO, Cs, Ta, Hf, Gd, Er and $^{207}Pb/^{204}Pb$ isotopic ratio in the final factor analysis.

The starting point of a factor analysis is a correlation matrix that is obtained by calculating the correlations between each pair of variables. The extraction of the factors is undertaken by calculating the eigenvalues of the correlation matrix. The number of positive eigenvalues determines the number of dimensions needed to describe the set of scores without losing information, and the number of the extracted factors (Rietveld and Van Hout, 1993). The construction of the factor is based on a transformation matrix that is given by the eigenvectors of the eigenvalues (Rietveld and Van Hout, 1993). Once the factors have been extracted, the factor loadings are calculated by correlating the original variables and the newly obtained factors. The first factor accounts for the maximum part of the variance, the second factor accounts for the maximum part of the remaining variance, and so on. In our case, seven factors (F) were extracted that account for ~84% of the cumulative variance (F1 22.7%; F2 18.6%; F3 12.2%; F4 11.8%; F5 6.4%; F6 6.4%; F7 6.1%) (**Table 1**).

The interpretation of the obtained factors can be problematic because the original variables have high loadings on the first factors as they account for the maximum part of the variance. To get around this problem, an orthogonal (Varimax) factor rotation is applied. Finally, each standardised variable score is multiplied by the corresponding standardised scoring coefficient, and the sum of these products results in the factor scores (Supplementary Material). It is noteworthy that in our case, the number of orogenic and anorogenic samples must be similar in order to avoid the dominance of one over another in extracting the main factors.

The factor scores are plotted in binary diagrams (Supplementary Material) in order to observe the variations affecting the samples in terms of controlling processes. Considering that the factors are the combination of all the variables used for the geochemical description and that each factor is standardised to a mean value of 0 and a

variance of 1, the intersection of the axes represents the mean of all the variables. For example, in the F2 vs. F1 diagram the intersection of the axes represents the point where the values of the variables, that are weighted by these two factors, coincide with their mean. Moving away from the axes intersection, the values of the variables will increase (positive side of the axes) or decrease (negative side of the axes) with respect to the mean.

4. Outcomes of the factor analysis

F1 is characterised by a positive correlation with K_2O, $^{87}Sr/^{86}Sr$, Rb, Sm and a group of highly mobile elements such as U, Th and Pb, and by a negative correlation with Fe_2O_3, CaO and $^{143}Nd/^{144}Nd$ (**Table 2**). F2 depends positively on Sr and Ba, as well as on some Light REE (LREE; La, Ce and Nd), Medium REE (MREE; Eu, Dy), and Y. F3 shows a positive correlation with TiO_2, MgO and P_2O_5 and a negative correlation with SiO_2 and Al_2O_3. F4 depends positively on Heavy REE (HREE) and Pr (LREE), as well as F5 on Na_2O, Zr and Nb. Note that, statistically, Pr is correlated with F4, although most of the LREE are associated with F2. Finally F6 and F7 depend positively on Pb isotopic ratios. F6 is correlated with $^{208}Pb/^{206}Pb$ and $^{207}Pb/^{206}Pb$, F7 to $^{206}Pb/^{204}Pb$ and $^{208}Pb/^{204}Pb$. By combining the seven factors in binary diagrams (Supplementary Material), we observed that the use of F1, F2, F3 and F5 explains the majority of the chemical variations of the samples. Fig. 3 shows the plots of the rotated component matrix expressed as binary diagrams of F2 vs. F1, F3 vs. F1 and F5 vs. F3. These plots help in understanding what variables influence the different factors more. On the other hand, in Fig. 4 and Fig. 5 we use the factor scores obtained for each sample in order to understand how the volcanic

rocks used in this study are related to the different factors (i.e., to the different original variable or chemical components).

On the whole, both orogenic and anorogenic samples show wide variations of all the factors (Fig. 4 and Supplementary Material). All the localities show a wide compositional range, in terms of both F1 and F2 (Fig. 5A and Fig. 5B), except Sardinia and Corsica (Sisco) (check legend of Figs. 1 and 5), for which only very few samples have been included in the factor analysis (3 and 1, respectively). The Central Mediterranean orogenic samples from Campania and the Aeolian Islands mostly straddle the zero axis intersection (Fig. 5A), indicating that the composition of these samples are close to the mean values of all variables included in F1 and F2. No correlation is found between composition and age, except some recent Campanian volcanic products shifting towards higher F1 values that are characterised by an increase in K_2O, Rb, Sm, U, Th and Pb contents, as well as radiogenic $^{87}Sr/^{86}Sr$. On the other hand, samples of the Roman Province, Western Alps and Tuscany, mostly plotting on the positive side of the x-axis, show alignments along different trends (Fig. 5A). Note that Tuscany samples include some rocks from Capraia but not from Elba Island. Three features can be highlighted: 1) Roman Province volcanic products show a very wide compositional range in terms of both F1 and F2, thus being characterised by an increase of K_2O, Rb, Sm, U, Th, Pb, and more radiogenic $^{87}Sr/^{86}Sr$, coupled with a decrease of Fe_2O_3 and CaO, and less radiogenic $^{143}Nd/^{144}Nd$, as well as by the enrichment in Sr, Ba, LREE, MREE, and Y contents; 2) All samples from Tuscany plot onto the negative side of the F2-axis, highlighting a lower content of Sr, Ba, LREE, MREE, and Y with respect to the Roman Province volcanics. One of the Tuscany lamproites shows a lower LREE content than the Roman province samples. At the same time, Tuscany samples show, similarly to the Roman Province, an increase of those elements related to F1, with

335 the highest contents observed in the lamproites. Western Alps samples plot between the
336 Roman and Tuscan provinces trends; 3) There is a temporal correlation of the volcanic
337 products of Tuscany, with the lamproites (4.1 Ma), associated with calc-alkaline, HK
338 calc-alkaline and shoshonitic rocks (0.88-1.35 Ma), being the first in the eruption
339 sequence (Ferrara and Tonarini, 1985; Conticelli et al., 2004; and references therein).

340 In the Westernmost Mediterranean (Fig. 5B), the orogenic samples of southern Spain,
341 Morocco and Alboran Basin (Fig. 1) are mostly aligned along a unique trend that starts
342 from slightly negative F1 and F2 values and evolves towards higher F1 and slightly
343 lower F2 values. Lamproites of southern Spain clearly plot outside this trend, between -
344 1 and +1 F2 values, and are characterised by the highest F1 values, indicating highest
345 K_2O, Rb, Sm, U, Th and Pb contents and the highest $^{87}Sr/^{86}Sr$, coupled with the lowest
346 Fe_2O_3 and CaO contents and the lowest $^{143}Nd/^{144}Nd$. Contrary to the case of the
347 Tuscany rocks, the association of Spanish volcanic rocks (lamproites, calc-alkaline, HK
348 calc-alkaline and shoshonitic rocks) is characterised by an opposite time sequence
349 (Conticelli et al., 2009a). In fact, lamproitic volcanism started later (8.08 - 6.37 Ma)
350 than the other subduction-related volcanic activity (14.4 - 6.2 Ma; Turner et al., 1999;
351 Duggen et al., 2004, 2005; and references therein).

352 Both Central and Western Mediterranean anorogenic rocks show the same F1 and F2
353 variations (light blue fields in Fig. 5A and Fig. 5B). The widest compositional range is
354 observed in the Upper Cretaceous rocks erupted in Portugal; all the others fall on the
355 negative side of F1. The major variation for these rocks is observed for Sr, Ba, LREE,
356 MREE, and Y contents (i.e., F2) and no age correlation is highlighted.

357 Fig. 3B, and consequently the values of the factor scores of Fig. 5C and Fig. 5D, give a
358 unique opportunity to observe the variation of all major elements at the same time

(except MnO, which is excluded from the factor analysis, and Na_2O, which is included in F5). Subduction-related volcanics mostly plot onto the negative side of the y-axis, i.e., they are usually characterised by low TiO_2, MgO, P_2O_5, and high SiO_2 and Al_2O_3, contents. Lamproites of both Central and Western Mediterranean show high values of F1 and F3, unlike all the other volcanic rocks. The samples of from the Central Western Mediterranean with intraplate affinity are characterised by a wide F3 variation, with a group of rocks showing the highest SiO_2 and Al_2O_3, and lowest TiO_2, MgO, P_2O_5 contents, mostly belonging to Palaeocene German and upper Cretaceous Portuguese suites.

A general tendency observed in Fig. 5E and Fig. 5F is that, as expected, the orogenic samples are mostly characterised by negative values of F5, i.e., lower Na_2O, Zr and Nb contents than the anorogenic rocks, which generally plot above the zero axes with Na_2O/K_2O ~1. Furthermore, subduction-related rocks of both Central and Western Mediterranean are aligned along a trend with factors F5 and F3 being inversely correlated. Lamproitic rocks are very well discriminated compared to other samples (light red field in Fig. 5E and Fig. 5F) and are characterised by a positive correlation of the factors F3 and F5, such that an increase of Na_2O, Zr and Nb is associated with an increase in TiO_2, MgO and P_2O_5, and a decrease of SiO_2 and Al_2O_3.

5. Mantle heterogeneities beneath the Mediterranean

Volcanic rocks are characterised by geochemical signatures that are typical of the environment in which they are produced. However, processes other than simple partial melting have to be accounted for in order to explain their geochemistry. These processes can be related to metasomatic and refertilisation events, due to fluid flow in the mantle.

383 Recycling of material due to subduction processes can also modify the mantle
384 composition, resulting in variations of the erupted volcanic products. In the Central and
385 Western Mediterranean, several recycling events of various continental/oceanic
386 subducted domains could have contaminated the lithospheric mantle for millions of
387 years (Fig. 6). These episodes can even go back to the Triassic and Permian periods,
388 and be related to the Variscan Orogeny and the subsequent Pangea Triassic rifting
389 processes that pre-date the Central Atlantic opening. Most of the geodynamic models
390 that have been proposed for the Central and westernmost Mediterranean (Tyrrhenian
391 area, the Alps, southern Spain, and northern Morocco) invoke the upwelling of
392 sublithospheric mantle. This upwelling would be responsible for the erupted anorogenic
393 suites, together with subduction-related rocks (Turner et al., 1999; Lustrino et al., 2004;
394 Duggen et al., 2005; Harangi et al., 2006) (Fig. 1).

395 The applied statistical approach permits identification of the major geochemical
396 components through the observation of a considerably smaller number of binary
397 diagrams, which are obtained by combining major and trace elements, and isotopic
398 ratios. In Fig. 4 and Fig. 5, orogenic and anorogenic rocks are rather well separated with
399 some overlapping regions, the orogenic samples being characterised by a great
400 compositional variability that highlights the heterogeneity of the mantle that is affected
401 by partial melting. When combining F1 and F2, or F1 and F3, various evolutionary
402 trends can be observed that affect the Roman Province, Tuscany or the Western Alps.
403 These trends reflect the recycling of material of different origins that were introduced
404 via subduction and metasomatised the pristine mantle that eventually melted. The two
405 end members represented by the Tuscan and Roman provinces are clearly related to the
406 different types of material that were brought down by the subducting slab, which
407 resulted in different petrographic and geochemical features of the erupted rocks. In the

408 case of the Roman Province, slab-derived melts have metasomatised a fertile mantle,
409 while in the case of Tuscany a harzburgitic mantle could have been metasomatised
410 through the subduction of continental crust or sediments (Avanzinelli et al., 2009). Both
411 provinces are characterised by an evolution of their volcanics towards potassic and
412 ultrapotassic end members. In the case of the Roman Province, the volcanic products
413 evolve from calc-alkaline to HK calc-alkaline and shoshonitic SiO_2-saturated (leucite-
414 free), to strongly SiO_2-undersaturated (with abundant leucite) tephrites, and to
415 phonolites (Peccerillo, 2005; Avanzinelli et al., 2009; Conticelli et al., 2009b). The
416 volcanic products from Tuscany evolve to ultrapotassic lamproites without leucite,
417 characterised by relatively high MgO and SiO_2 with crustal isotopic signature
418 (Conticelli et al., 2009a, and references therein).

419 The benefits of the statistical approach in geochemical investigation is provided by the
420 discrimination of the orogenic and anorogenic fields, as well as that of the lamproitic
421 rocks. Other evidence in favour of the proposed approach is provided by the
422 combination of the elements within each factor. The positive correlation between K_2O
423 and Rb or U-Th-Pb, as well as the negative correlation between the $^{87}Sr/^{86}Sr$ and
424 $^{143}Nd/^{144}Nd$ isotopic ratios on F1, are clear examples. The negative correlation between
425 MgO and SiO_2-Al_2O_3 recorded also by F3, or the dependence of F4 almost entirely on
426 HREE further confirm the appropriateness of the approach. Supporting evidence is,
427 finally, also given by F6 and F7 depending on to $^{208}Pb/^{206}Pb$ - $^{207}Pb/^{206}Pb$, and
428 $^{206}Pb/^{204}Pb$ - $^{208}Pb/^{204}Pb$, respectively.

429

430 ## 6. Volcanic activity and the double polarity subduction model

Geodynamic models that have been proposed for the evolution of the westernmost Mediterranean are mainly based on geologic and seismologic evidences, as well as on petrography and exhumation ages of metamorphic units that compose the inner parts of the Betic-Rif arc. Many of these models are poorly constrained from a volcanological point of view, and volcanic activity is not only used as a key constraint but also as a corollary. The complexity in interpreting the volcanic geochemistry in this region is basically related to the long-term recycling of material, coupled to depletion events caused by partial melting due to subduction or rifting phases (Fig. 6). The modifications of the Mediterranean mantle are, therefore, reflected in the volcanic products, whose geochemical features do not always correspond to the present-day geodynamic environment in which they are sampled (see also Lustrino and Wilson, 2007; Lustrino et al., 2011; Carminati et al., 2012).

Here, we analyse the geochemical characteristics of the volcanic rocks in the framework of the recent geodynamic model proposed by Vergés and Fernàndez (2012) for the westernmost Mediterranean. These authors propose the existence of two opposite dipping slabs (Fig. 6), which retreated in opposite directions (Fig. 7), based on four key premises related to: 1) the large-scale plate reconstructions addressing the Africa–Iberia plate boundary during the Mesozoic and the Cenozoic; 2) the geographic distribution of HP/LT metamorphic rocks of the inner orogeny located along the Alboran and the Algerian margins; 3) the role of mechanical stratigraphy of the Iberia paleo-margin, where the External Units are separated from the Internal Betic–Rif units through Triassic detachment levels; and 4) the timing of onset of compressional deformation along the Betic–Rif system.

This model includes seven time-steps or stages. The first stage is related to the onset of the Africa-Iberia convergence at about 85 Ma, and volcanic activity is restricted to

southwest Iberia far from the Ligurian-Tethys domain. The second stage (middle Eocene, 47-42 Ma) takes into account a HP/LT metamorphic peak (recorded in the Nevado-Filabride complex) related to SE subduction beneath northern Africa. During this stage, no volcanic activity is reported in the westernmost Mediterranean, but some anorogenic volcanic rocks occurred in the High Atlas that are probably unrelated with subduction (at Tamazert and Rekkam; Bouabdli et al., 1988; Bernard-Griffiths et al., 1991; Bouabdli and Liotard, 1992; Rachdi et al., 1997; Duggen et al., 2005).

In the third stage (Oligocene, 30-25 Ma), the roll-back phase and the exhumation of the HP/LT Ligurian-Tethys metamorphic rocks began. The earliest magmatic manifestation is represented by the intrusion of tholeiitic Malaga dykes, dated 33.6±0.6 Ma (Duggen et al., 2004) and 30.2±0.9 Ma (Turner et al., 1999). Younger ages ranging from 23 to 17 Ma have been reported by several authors (e.g., Torres-Roldán et al., 1986; Turner et al., 1999; Duggen et al., 2004), coinciding with metamorphic events dated 22-17 Ma (Priem et al., 1979; Monié et al., 1994; Kelley and Platt, 1999). These young volcanic ages (23-17 Ma) are related to a thermal event that reset the system, rather than being related to the magma ascent and dykes emplacement (Duggen et al., 2004; Platt et al., 2013). The tholeiitic Malaga dykes are characterised by moderate Fe enrichment (Turner et al., 1999). These rocks show crustal contamination, indicated by small negative Ta-Nb, Ti and Zr-Hf anomalies, positive Rb, U, K and Pb anomalies, higher $^{87}Sr/^{86}Sr$, and lower $^{143}Nd/^{144}Nd$ relative to the depleted mantle, and elevated $^{208}Pb/^{204}Pb$ and $^{207}Pb/^{204}Pb$. However, the least contaminated samples show relative low Fe and high Si contents, flat REE patterns, and high HREE concentrations, indicating that partial melting did not take place in the presence of garnet. Turner et al. (1999) calculated that 10-15% of mantle partial was melting in the spinel stability field (less than 60-70 km). This feature allows us to place the genesis of these melts as due to

partial melting of a mantle wedge (Duggen et al., 2004), most probably enriched in incompatible elements through the percolation of fluids coming from the subducting slab and involving a sedimentary component, in agreement with the third stage, described by Vergés and Fernàndez (2012). Note that the Malaguide Complex corresponds to the upper plate and it has been tectonically transported to its present position as a consequence of the slab roll-back.

The fourth stage, dated as late Oligocene-early Miocene (27-20 Ma), is characterised by a progressive northwest and westward displacement of the trench resulting in an arcuate subducting slab with a SE to E-dipping polarity and the opening of the Alboran back-arc basin. The absence of volcanic activity is a key feature of this stage, although volcanism will sporadically reappear a few million years later. Cordierite-bearing dacite samples in the Mar Menor area have been dated at around 18.5±1.6 Ma (Duggen et al., 2004). These anatectic melts have been also reported by Zeck et al. (1999) and are explained as melting of pelitic to quartz-feldspatic clastic rocks originated in a slab detachment setting. This hypothesis is well correlated with the fifth stage, which is characterised by the end of major extension in the Alboran Basin (18-16 Ma) and the onset of slab tear and E-W extension in the Eastern Betics. The occurrence of some calc-alkaline products in the Alboran Sea (ODP 977 at ~17.6 Ma; Duggen et al., 2004) is related to the active slab retreating in the West Alboran Basin, as proposed by the model.

Most of the volcanic activity of the western Mediterranean occurred since ~15-14 Ma (hereinafter, all age datings refer to the data of Duggen et al., 2004, and references therein). During the Middle to Early Miocene, subduction-related volcanic rocks with tholeiitic to HK calc-alkaline affinity had erupted in different localities: in Ras Tarf (northern Morocco) and Cabo de Gata (southern Spain) at ~15 Ma, in the Alboran Sea

(ODP 978) around 13 Ma, in Oranie (Northern Algeria) and the Yusuf Ridge (Alboran Sea) at ~11 Ma, and in the Alboran Ridge at ~10 Ma. This volcanism continued between ~9 and ~7 Ma, producing volcanic rocks with a typical subduction signature in the Alboran Sea (the tholeiitic/calc-alkaline volcanism of Mansour Smt. at ~9 Ma) and Northern Algeria (at Gourougou and Trois Furches with calc-alkaline affinity, ~9 Ma). In southern Spain, rocks with calc-alkaline affinity erupted at ~8 Ma in Murcia and Mazarron (with the occurrence of alkaline rocks with sodic affinity in the area of Picassent; Ancochea and Huertas, 2002). Following the stage 6 in Vergés and Fernàndez (2012), this orogenic volcanism is interpreted as the partial melting of the mantle wedge that is related to the W-directed slab roll-back affecting mainly the western part of the Betic-Rif-Alboran system.

The last volcanic phase occurred in the late Miocene-Quaternary periods and comprises a wide range of volcanic products. The peculiarity of this period is the eruption of sodic alkaline (anorogenic) rocks soon after the emplacement of volcanics with typical subduction-related signature. In the area of Guilliz (north Morocco), calc-alkaline products erupted at ~7 Ma are followed after only ~1 My by sodic alkaline rocks. At Gourougou and Trois Furches (north Morocco), the same evolution between orogenic and anorogenic igneous rocks is observed (Maury et al., 2000). Anorogenic rocks erupted from ~3 Ma in the area of Oujda and Oranie (northern Algeria; Coulon et al., 2002). Along the Iberian margin, calc-alkaline and HK calc-alkaline rocks were erupted during the late Miocene-Quaternary, especially along the Murcia-Almeria coast. Lamproite-like ultrapotassic rocks (8.08-6.37 Ma) were erupted in the area of Vera, Cancarix, Fortuna and Jumilla, some of which emplaced along transform faults (e.g., the Socovos fault, Pérez-Valera et al., 2013). These rocks are usually interpreted as originated by the partial melting of a strongly metasomatised mantle. Sediments play an

531 important role in the generation of the lamproitic products. If the subducting slab is
532 carrying a large quantity of sediments to the mantle, they will deeply metasomatise the
533 mantle wedge by adding incompatible elements (Ba, Rb, Sr, Th) and K_2O, precipitating
534 clinopyroxene, phlogopite and amphibole either as small veins (Foley, 1992) or
535 disseminated in the peridotitic matrix (Coltorti et al., 2004). On the other hand,
536 Bianchini et al. (2015) link the source of the Spanish lamproites to a widespread
537 igneous veining (norite veins) observable in composite mantle xenoliths from Tallante,
538 coupled with very refractory peridotite compositions, known from xenolith occurrences
539 in the Iberian margin (Bianchini et al., 2007). According to those authors, the
540 metasomatism has to account for processes related to Cenozoic and Paleozoic times.
541 The final magmatic input in southern Spain is represented by the alkaline products of
542 Tallante, erupted between 2.93 Ma and 2.29 Ma (Cebriá et al., 2009).

543 The Late Miocene-Quaternary volcanic phase in the western Mediterranean is poorly
544 integrated in the double polarity subduction model. The eruption of the calc-alkaline
545 and HK calc-alkaline rocks is in agreement with a subduction process that is in its
546 mature stage (no retreating or active subduction), as proposed by Vergés and Fernàndez
547 (2012) in stage 7. In northern Africa (Morocco and west Algeria), the sodic alkaline
548 volcanic episodes following the typical subduction-related products can be mainly
549 ascribed to three mechanisms: i) sublithospheric flow, as evidenced from mantle
550 anisotropy analysis (Diaz et al., 2010, 2015); ii) slab break-off, as also proposed for the
551 alkaline products of the intra-Apennines volcanism by Bianchini et al. (2008); or iii)
552 splash-plume effect (Davies and Bunge, 2006) due to convective instabilities, as has
553 been also proposed by Beccaluva et al. (2011) for Sardinia and Calatrava (southern
554 Spain) volcanism. Furthermore, the occurrence of anorogenic rocks in Tallante is an
555 additional evidence of the lateral tear responsible of the uplift of the eastern part of the

556 Betics (e.g., Spakman and Wortel, 2004; García-Castellanos and Villaseñor, 2011;
557 Mancilla et al., 2015) as has been included in the model by Vergés and Fernàndez
558 (2012).

559

560 7. Conclusions

561 We applied a multi-factor statistical approach to a large and well-studied geochemical
562 dataset of volcanic rocks in the central and western Mediterranean with the aim to
563 reproduce the main petrological characteristics that were previously observed with
564 bivariate diagrams. The main advantage of this method is that it allows the investigation
565 of the processes that are responsible for the geochemical signature of the studied
566 volcanic rock suites in a fast and simple way. This is possible through the statistical
567 determination of the main controlling factors that are constructed by using the original
568 geochemical elements. The method has the drawback of losing part of the information
569 when extracting the factors, thus limiting a detailed interpretation. However, any
570 methodology has its own advantages and drawbacks, hence factor analysis must be
571 considered as a complementary method to classical bivariate diagrams in order to
572 extract all the information contained in the geochemical datasets.

573 Keeping these considerations in mind, the main concluding remarks from the presented
574 study are:

575 1. After filtering for common geochemical data, the original datasets that encompassed
576 a total of ~7,000 orogenic and ~7,800 anorogenic analyses, were reduced to 283
577 orogenic and 310 anorogenic volcanic samples.

2. The factor analysis performed using the PCA method reduced the original 36 geochemical parameters, expressed as oxides, elements or isotopic ratios, to seven factors, accounting for ~84% of variance.

3. Despite the existing overlap between anorogenic and orogenic geochemical fields, factor analysis discriminates between these two rock types rather well.

4. Lamproites always plot in a separate field, emphasising the great compositional difference among the western and central Mediterranean volcanic rocks, and the huge sediment recycling in the mantle that is responsible for the origin of these exotic rocks.

5. Factor analysis evidences mantle metasomatic processes that are responsible for compositional heterogeneities. The controlling factors are related to mantle wedge percolation of fluids from the subducting slab, and high sediment recycling.

6. The double polarity subduction model that is proposed to explain the evolution of the westernmost Mediterranean is compatible with the timing and type of volcanic rocks and supported by the controlling processes that are highlighted with the factor analysis.

7. The close relationships between the tectonic processes responsible for the generation of the erupted volcanic rocks in the westernmost Mediterranean region and their different geochemical signatures are yet to become well established, thus demanding further multidisciplinary efforts.

Acknowledgements

The present work has been supported by the research projects WEME (CSIC-201330E111) and MITE (CGL2014-59516-P). We gratefully acknowledge two

600 anonymous reviewers for their constructive comments that greatly improved the first
601 version of the manuscript.

References

Alvarez, W., Cocozza, T., Wezel, F.C., 1974. Fragmentation of the Alpine orogenic belt by microplate dispersal. Nature 248, 309-314.

Alvarez, W., Shimabukuro, D.H., 2009. The geological relationships between Sardinia and Calabria during Alpine and Hercynian times. Bollettino della Societa Geologica Italiana 128, 257-268.

Ancochea, E., Huertas, M.J., 2003. Nuevos datos geocronológicos y geoquímicos de las manifestaciones volcánicas de Picasent y Cofrentes (Valencia). Geogaceta 32, 31-35.

Araña, V., Aparicio, A., Martin Escorza, C., Garcia Cacho, L., Ortiz, R., Vaquer, R., Barberi, F., Ferrara, G., Albert, J., Gassiot, X., 1983. El volcanismo neogeno-cuaternario de Catalunya: caracteres estructurales, petrologicos y geodinámicos. Acta Geològica Hispànica 18, 1-17.

Avanzinelli, R., Lustrino, M., Mattei, M., Melluso, L., Conticelli, S., 2009. Potassic and ultrapotassic magmatism in the circum-Tyrrhenian region: significance of carbonated pelitic vs. pelitic sediment recycling at destructive plate margins. Lithos 113, 213-227.

Ayala, C., Torne, M., Pous, J., 2003. The lithosphere-asthenosphere boundary in the Western Mediterranean: Results from 3D gravity and geoid modeling. Earth and Planetary Science Letter, 209, 275-290.

Beccaluva, L., Bianchini, G., Bonadiman, C., Siena, F., Vaccaro, C., 2004. Coexisting anorogenic and subduction-related metasomatism in mantle xenoliths from the Betic Cordillera (southern Spain). Lithos 75, 67-87.

Beccaluva, L., Bianchini, G., Mameli, P., Natali, C., 2013. Miocene shoshonite volcanism in Sardinia: Implications for magma sources and geodynamic evolution of the central-western Mediterranean. Lithos 180-181, 128-137.

Beccaluva, L., Bianchini, G., Natali, C., Siena, F., 2011. Geodynamic control on orogenic and anorogenic magmatic phases in Sardinia and Southern Spain: inferences for the Cenozoic evolution of the western Mediterranean. Lithos 123, 218-224.

Bernard-Griffiths, J., Fourcade, S., Dupuy, C., 1991. Isotopic study (Sr, Nd, O and C) of lamprophyres and associated dykes from Tamazert (Morroco): crustal contamination processes and source characteristics. Earth and Planetary Science Letters 103, 190-199.

Bezada, M.J., Humphreys, E.D., Toomey, D.R., Harnafi, M., Dávila, J.M., Gallart, J., 2013. Evidence for slab roll-back in westernmost Mediterranean from improved upper mantle imaging. Earth and Planetary Science Letters 368, 51-60.

Bianchini, G., Beccaluva, L., Bonadiman, C., Nowell, G., Pearson, G., Siena, F., Wilson, M., 2007. Evidence of diverse depletion and metasomatic events in harzburgite–lherzolite mantle xenoliths from the Iberian plate (Olot, NE Spain): implications for lithosphere accretionary processes. Lithos 94, 25–45.

Bianchini, G., Beccaluva, L., Siena, F., 2008. Subduction-related and intraplate Cenozoic volcanism in the rifted Apennines/Adriatic domain. Lithos 101, 125-140.

641 Bianchini, G., Braga, R., Langone, A., Natali, C., Tiepolo, M., 2015. Metasedimentary
642 and igneous xenoliths from Tallante (Betic Cordillera, Spain): inferences on crust-
643 mantle interactions and clues for post-collisional volcanism magma sources. Lithos 220-
644 223, 191-199.

645 Bird, P., 1979. Continental delamination and the Colorado Plateau. Journal of
646 Geophysical Reseach 84, 7561-7571.

647 Boccaletti, M., Guazzone, G., 1974. Remnant arcs and marginal basins in the Cainozoic
648 development of the Mediterranean. Nature 252, 18-21.

649 Bonnin, M., Nolet, G., Villaseñor, A., Gallart, J., Thomas, C., 2014. Multiple-frequency
650 tomography of the upper mantle beneath the African/Iberian collision zone.
651 Geophysical Journal International 198, 1458-1473.

652 Booth-Rea, G., Ranero, C.R., Martínez-Martínez, J.M., Grevemeyer, I., 2007. Crustal
653 types and Tertiary tectonic evolution of the Alborán sea, western Mediterranean.
654 Geochemistry, Geophysics, Geosystems 8, Q10005.

655 Bouabdli, A., Dupuy, C., Dostal, J., 1988. Geochemistry of Mesozoic alkaline
656 lamprophyres and related rocks from the Tamazert massif, High Atlas (Morocco).
657 Lithos 22, 43-58.

658 Bouabdli, A., Liotard, J.M., 1992. Kimberlite affinities of the ultrabasic lamprophyres
659 of the Tamazert carbonatite massif, Moroccan High Atlas. Comptes Rendus - Academie
660 des Sciences, Serie II 314, 351-357.

661 Carballo, A., Fernandez, M., Torne, M., Jiménez-Munt, I., Villaseñor, A., 2015.
662 Thermal and petrophysical characterization of the lithospheric mantle along the
663 northeastern Iberia geo-transect. Gondwana Research 27, 1430-1445.

664 Carminati, E., Doglioni, C., 2004. Mediterranean Tectonics, Encyclopedia of Geology.
665 Elsevier, pp. 135-146.

666 Carminati, E., Lustrino, M., Doglioni, C., 2012. Geodynamic evolution of the central
667 and western Mediterranean: Tectonics vs. igneous petrology constraints.
668 Tectonophysics 579, 173-192.

669 Casciello, E., Fernàndez, M., Vergés, J., Cesarano, M., Torne, M., 2015. The Alboran
670 domain in the western Mediterranean evolution: The birth of a concept. Bulletin de la
671 Societe Geologique de France 186, 371-384.

672 Cebriá, J.M., López-Ruiz, J., 1995. Alkali basalts and leucitites in an extensional
673 intracontinental plate setting: the late Cenozoic Calatrava Volcanic Province (central
674 Spain). Lithos 35, 27-46.

675 Cebriá, J.M., López-Ruiz, J., Carmona, J., Doblas, M., 2009. Quantitative petrogenetic
676 constraints on the Pliocene alkali basaltic volcanism of the SE Spain Volcanic Province.
677 Journal of Volcanology and Geothermal Research 185, 172-180.

678 Chiarabba, C., Giacomuzzi, G., Bianchi, I., Agostinetti, N.P., Park, J., 2014. From
679 underplating to delamination-retreat in the northern Apennines. Earth and Planetary
680 Science Letters 403, 108-116.

681 Coltorti, M., Beccaluva, L., Bonadiman, C., Faccini, B., Ntaflos, T., Siena, F., 2004.
682 Amphibole genesis via metasomatic reaction with clinopyroxene in mantle xenoliths
683 from Victoria Land, Antarctica. Lithos 75, 115-139.

684 Comas, M.C., García-Dueñas, V., Jurado, M.J., 1992. Neogene tectonic evolution of the
685 Alboran Sea from MCS data. Geo-Marine Letters 12, 157-164.

686 Comas, M.C., Platt, J.P., Soto, J.I., Watts, A.B., 1999. The origin and tectonic history of
687 the Alboran basin: insights from LEG 161 results, in: Zahn, R., Comas, M.C., Klaus, A.
688 (Eds.), Proceedings of the Ocean Drilling Program, Scientific Results, pp. 555-580.

689 Conticelli, S., Guarnieri, L., Farinelli, A., Mattei, M., Avanzinelli, R., Bianchini, G.,
690 Boari, E., Tommasini, S., Tiepolo, M., Prelević, D., Venturelli, G., 2009a. Trace
691 elements and Sr–Nd–Pb isotopes of K-rich, shoshonitic, and calc-alkaline magmatism
692 of the Western Mediterranean Region: genesis of ultrapotassic to calc-alkaline
693 magmatic associations in a post-collisional geodynamic setting. Lithos 107, 68-92.

694 Conticelli, S., Marchionni, S., Rosa, D., Giordano, G., Boari, E., Avanzinelli, R., 2009b.
695 Shoshonite and sub-alkaline magmas from an ultrapotassic volcano: Sr–Nd–Pb isotope
696 data on the Roccamonfina volcanic rocks, Roman Magmatic Province, Southern Italy.
697 Contrib Mineral Petrol 157, 41-63.

698 Conticelli, S., Melluso, L., Perini, G., Avanzinelli, R., Boari, E., 2004. Petrologic,
699 geochemical and isotopic characteristics of potassic and ultrapotassic magmatism in
700 central-southern Italy: inferences on its genesis and on the nature of mantle sources.
701 Periodico di Mineralogia 73, 135-164.

702 Coulon, C., Megartsi, M.h., Fourcade, S., Maury, R.C., Bellon, H., Louni-Hacini, A.,
703 Cotten, J., Coutelle, A., Hermitte, D., 2002. Post-collisional transition from calc-
704 alkaline to alkaline volcanism during the Neogene in Oranie (Algeria): magmatic
705 expression of a slab breakoff. Lithos 62, 87-110.

706 Dal Piaz, G.V., Bistacchi, A., Massironi, M., 2003. Geological outline of the Alps.
707 Episodes 26, 175-180.

708 Davies, J.H., Bunge, H.P., 2006. Are splash plumes the origin of minor hotspots?
709 Geology 34, 349-352.

710 Devoti, R., Riguzzi, F., Cuffaro, M., Doglioni, C., 2008. New GPS constraints on the
711 kinematics of the Apennines subduction. Earth and Planetary Science Letters 273, 163-
712 174.

713 Dewey, J.F., Helman, M.L., Knott, S.D., Turco, E., Hutton, D.H.W., 1989. Kinematics
714 of the western Mediterranean. Geological Society, London, Special Publications 45,
715 265-283.

716 Díaz, J., Gallart, J., Morais, I., Silveira, G., Pedreira, D., Pulgar, J.A., Dias, N.A., Ruiz,
717 M., González-Cortina, J.M., 2015. From the Bay of Biscay to the High Atlas:

completeng the anisotropic characterization of the upper mantle beneath the westernmost Mediterranean region. Tectonophysics 663, 192-202.

Díaz, J., Pedreira, D., Ruiz, M., Pulgar, J.A., Gallart, J., 2012. Mapping the indentation between the Iberian and Eurasian plates beneath the Western Pyrenees/Eastern Cantabrian Mountains from receiver function analysis. Tectonophysics 570-571, 114-122.

Diaz, J., Gallart, J., Villaseñor, A., Mancilla, F., Pazos, A., Córdoba, D., Pulgar, J.A., Ibarra, P., Harnafi, M., 2010. Mantle dynamics beneath the Gibraltar Arc(western Mediterranean) from shear-wave splitting measurementson a dense seismic array. Geophysical Research Letters 37, L18304.

Doblas, M., López-Ruiz, J., Cebriá, J.M., 2007. Cenozoic evolution of the Alboran Domain: a review of the tectonomagmatic models. Special Paper of the Geological Society of America 418, 303-320.

Doglioni, C., Innocenti, F., Morellato, C., Procaccianti, D., Scrocca, D., 2004. On the Tyrrhenian sea opening. Memorie descrittive della carta geologica d'Italia 44, 147-164.

Duggen, S., Hoernle, K., Van Den Bogaard, P., Garbe-Schönberg, D., 2005. Post-collisional transition from subduction- to intraplate-type magmatism in the westernmost Mediterranean: evidence for continental-edge delamination of subcontinental lithosphere. Journal of Petrology 46, 1155-1201.

Duggen, S., Hoernle, K., van den Bogaard, P., Harris, C., 2004. Magmatic evolution of the Alboran region: the role of subduction in forming the western Mediterranean and causing the Messinian Salinity Crisis. Earth and Planetary Science Letters 218, 91-108.

El Azzouzi, M., Bellon, H., Coutelle, A., Réhault, J.P., 2014. Miocene magmatism and tectonics within the Peri-Alboran orogen (western Mediterranean). Journal of Geodynamics 77, 171-185.

El Azzouzi, M., Bernard-Griffiths, J., Bellon, H., Maury, R.C., Piqué, A., Fourcade, S., Cotten, J., Hernandez, J., 1999. Évolution des sources du volcanisme marocain au cours du Néogène. Earth and Planetary Science 329, 95-102.

Faccenna, C., Becker, T.W., Auer, L., Billi, A., Boschi, L., Brun, J.P., Capitanio, F.A., Funiciello, F., Horvàth, F., Jolivet, L., Piromallo, C., Royden, L., Rossetti, F., Serpelloni, E., 2014. Mantle dynamics in the Mediterranean. Reviews of Geophysics 52, 283-332.

Faccenna, C., Piromallo, C., Crespo-Blanc, A., Jolivet, L., Rossetti, F., 2004. Lateral slab deformation and the origin of the western Mediterranean arcs. Tectonics 23, 1-21.

Faccenna, C., Mattei, M., Funiciello, R., Jolivet, L., 1997. Styles of back-arc extension in the Central Mediterranean. Terra Nova 9, 126-130.

Ferrara, G., Tonarini, S., 1985. Radiometric geochronology in Tuscany: results and problems. Rendiconti della Società Geologica Italiana di Mineralogia e Petrologia 40, 111-124.

757 Fichtner, A., Villaseñor, A., 2015. Crust and upper mantle of the western Mediterranean
758 - Constraints from full-waveform inversion. Earth and Planetary Science Letters 428,
759 52-62.

760 Foley, S., 1992. Vein-plus-wall-rock melting mechanisms in the lithosphere and the
761 origin of potassic alkaline magmas. Lithos 28, 435-453.

762 Frizon de Lamotte, D., Saint Bezar, B., Bracène, R., Mercier, E., 2000. The two main
763 steps of the Atlas building and geodynamics of the western Mediterranean. Tectonics
764 19, 740-761.

765 García-Castellanos, D., Villaseñor, A., 2011. Messinian salinity crisis regulated by
766 competing tectonics and erosion at the Gibraltar arc. Nature 480, 359-363.

767 García-Dueñas, V., Balanyá, J.C., Martínez-Martínez, J.M., 1992. Miocene extensional
768 detachments in the outcropping basement of the northern Alboran Basin (Betics) and
769 their tectonic implications. Geo-Marine Letters 12, 88-95.

770 Giacomuzzi, G., Civalleri, M., De Gori, P., Chiarabba, C., 2012. A 3D Vs model of the
771 upper mantle beneath Italy: Insight on the geodynamics of central Mediterranean. Earth
772 and Planetary Science Letters 335-336, 105-120.

773 Gutscher, M.-A., Malod, J., Rehault, J.-P., Contrucci, I., Klingelhoefer, F., Mendes-
774 Victor, L., Spakman, W., 2002. Evidence for active subduction beneath Gibraltar.
775 Geology 30, 1071-1074.

776 Harangi, H., Downs, H., Seghedi, I., 2006. Tertiary–Quaternary subduction processes
777 and related magmatism in the Alpine–Mediterranean region. Geological Society
778 Memoir 32, 167-190.

779 Jiménez-Munt, I., Fernàndez, M., Vergés, J., Afonso, J.C., Garcia-Castellanos, D.,
780 Fullea, J., 2010. Lithospheric structure of the Gorringe Bank: insights into its origin and
781 tectonic evolution. Tectonics 29, TC5019.

782 Jolivet, L., Faccenna, C., 2000. Meditterranean extension and the Africa-Eurasia
783 collision. Tectonics 19, 1095-1106.

784 Kelley, S.P., Platt, J.P., 1999. Ar-Ar dating of biotite and muscovite from Alboran
785 basement samples, site 976. Proceedings of the Ocean Drilling Program: Scientific
786 Results 161, 301-305.

787 Lonergan, L., White, N., 1997. Origin of the Betic-Rif mountain belt. Tectonics 16,
788 504-522.

789 Lustrino, M., 2011. What 'anorogenic' igneous rocks can tell us about the chemical
790 composition of the upper mantle: case studies from the circum-Mediterranean area.
791 Geological Magazine 148, 304-316.

792 Lustrino, M., Wilson, M., 2007. The circum-Mediterranean anorogenic Cenozoic
793 igneous province. Earth-Science Reviews 81, 1-65.

Lustrino, M., Duggen, S., Rosenberg, C.L., 2011. The Central-Western Mediterranean: anomalous igneous activity in an anomalous collisional tectonic setting. Earth-Science Reviews 104, 1-40.

Lustrino, M., Morra, V., Melluso, L., Brotzu, P., D'Amelio, F., Fedele, L., Franciosi, L., Lonis, R., Lieberckнecht, A.M.P., 2004. The Cenozoic igneous activity of Sardinia. Periodico di Mineralogia 73, 105-134.

Mancilla, F.L., Booth-Rea, G., Stich, D., Pérez-Peña, J.V., Morales, J., Azañón, J.M., Martin, R., Giaconia, F., 2015. Slab rupture and delamination under the Betics and Rif constrained from receiver functions. Tectonophysics 663, 225-237.

Martí, J., Mitjavila, J., Roca, E., Aparicio, A., 1992. Cenozoic magmatism of the Valencia Trough (western Mediterranean): relationship between structural evolution and volcanism. Tectonophysics 203, 145-165.

Maury, R., Fourcade, S., Coulon, C., El Azzouzi, M.h., Bellon, H., Coutelle, A., Ouabadi, A., Semroud, B., Megartsi, M.h., Cotten, J., Belanteur, O., Louni-Hacini, A., Piqué, A., Capdevila, R., Hernandez, J., Réhault, J.-P., 2000. Post-collisional Neogene magmatism of the Mediterranean Maghreb margin: a consequence of slab breakoff. Comptes Rendus de l'Académie des Sciences - Series IIA - Earth and Planetary Science 331, 159-173.

Mazzoli, S., Helman, M., 1994. Neogene patterns of relative plate motion for Africa-Europe: some implications for recent central Mediterranean tectonics. Geologische Rundschau 83, 464-468.

Miller, M.S., Allam, A.A., Becker, T.W., Di Leo, J.F., Wookey, J., 2013. Constraints on the tectonic evolution of the westernmost Mediterranean and northwestern Africa from shear wave splitting analysis. Earth and Planetary Science Letters 375, 234-243.

Monié, P., Torres-Roldán, R.L., García-Casco, A., 1994. Cooling and exhumation of the Western Betic Cordilleras, $^{40}Ar/^{39}Ar$ thermochronological constraints on a collapsed terrane. Tectonophysics 238, 353-379.

Palomeras, I., Thurner, S., Levander, A., Liu, K., Villasenor, A., Carbonell, R., Harnafi, M., 2014. Finite-frequency Rayleigh wave tomography of the western Mediterranean: mapping its lithospheric structure. Geochemistry, Geophysics, Geosystems 15, 140-160.

Peccerillo, A., 2005. Plio-Quaternary volcanism in Italy. Springer, Heidelberg 1-365.

Pérez-Valera, L.A., Rosenbaum, G., Sánchez-Gómez, M., Azor, A., Fernández-Soler, J.M., Pérez-Valera, F., Vasconcelos, P.M., 2013. Age distribution of lamproites along the Socovos Fault (southern Spain) and lithospheric scale tearing. Lithos 180-181, 252-263.

Piromallo, C., Morelli, A., 2003. P wave tomography of the mantle under the Alpine-Mediterranean area. Journal of Geophysical Research: Solid Earth 108, 1-23.

Platt, J.P., Behr, W.M., Johanesen, K., Williams, J.R., 2013. The Betic-Rif Arc and its orogenic hinterland: a review. Annual Review of Earth and Planetary Sciences 41, 313-357.

834 Priem, H.N.A., Boelrijk, N.A.I.M., Hebeda, E.H., Oen, I.S., Verdurmen, E.A.T.,
835 Verschure, R.H., 1979. Isotopic dating of the emplacement of the ultramafic masses in
836 the Serrania de Ronda, Southern Spain. Contribution to Mineralogy and Petrology 70,
837 103-109.

838 Rabinowitz, P.D., LaBrecque, J., 1979. The Mesozoic South Atlantic Ocean and
839 evolution of its continental margins. Journal of Geophysical Research: Solid Earth 84,
840 5973-6002.

841 Rachdi, H., Berrahma, M.H., Delaloye, M., Faure-Muret, A., Dahmani, M., 1997. Le
842 volcanisme tertiare du Rekkame (Maroc): pétrologie, géochimie et géochronologie.
843 Journal of African Earth Sciences 24, 259-269.

844 Reimann, C., Filzmoser, P., Garrett, R.G., 2002. Factor analysis applied to regional
845 geochemical data: problems and possibilities. Applied Geochemistry 17, 185-206.

846 Rietveld, T., Van Hout, R., 1993. Statistical techniques for the study of language and
847 language behaviour. Berlin: Mouton de Gruyter.

848 Roca, E., Frizon de Lamotte, D., Mauffret, A., Bracène, R., Vergés, J., Benaouali, N.,
849 Fernàndez, M., Muñoz, J.A., Zeyen, H., 2004. Transect II: Aquitaine Basin – Pyrenees
850 – Ebro Basin – Catalan Range – Valencia Trough – Balearic Block – Algerian Basin –
851 Kabylies – Atlas – Sahara Platform. In: The TRANSMED Atlas. The Mediterranean
852 Region from Crust to Mantle, Cavazza, W., Roure, F., Spakman, W., Stampfli, G.M.
853 and Ziegler, P.A. (Eds.). Springer-Verlag, Berlin, ISBN: 3-540-22181-6, 141 pp.

854 Rosenbaum, G., Lister, G.S., Duboz, C., 2002a. Reconstruction of the tectonic evolution
855 of the western Mediterranean since the Oligocene. Journal of the Virtual Explorer 8,
856 107-126.

857 Rosenbaum, G., Lister, G.S., Duboz, C., 2002b. Relative motions of Africa, Iberia and
858 Europe during Alpine orogeny. Tectonophysics 359, 117-129.

859 Rosenbaum, G., Lister, G.S., 2004. Formation of arcuate orogenic belts in the western
860 Mediterranean region. In: Sussman, A.J., Weil, A.B. (Eds.), Orogenic curvature:
861 integrating paleomagnetic and structural analyses: Boulder, Colorado, Geological
862 Society of America Special Paper, 383, pp. 41–56.

863 Schettino, A., Turco, E., 2006. Plate kinematics of the western Mediterranean region
864 during the Oligocene and Early Miocene. Geophysical Journal International 166, 1398-
865 1423.

866 Simancas, J.F., Tahiri, A., Azor, A., Lodeiro, F.G., Martínez Poyatos, D.J., El Hadi, H.,
867 2005. The tectonic frame of the Variscan–Alleghanian orogen in Southern Europe and
868 Northern Africa. Tectonophysics 398, 181-198.

869 Soto, J.I., Fernández-Ibáñez, F., Fernàndez, M., García-Casco, A., 2008. Thermal
870 structure of the crust in the Gibraltar arc: influence on active tectonics in the western
871 Mediterranean. Geochemistry, Geophysics, Geosystems 9, Q10011.

872 Spakman, W., Wortel, R., 2004. A tomographic view on western Mediterranean
873 geodyamics. The TRANSMED Atlas: The Mediterranean Region from Crust to Mantle,
874 31-52.

875 Thurner, S., Palomeras, I., Levander, A., Carbonell, R., Lee, C., 2014. Ongoing
876 lithospheric removal in the western Mediterranean: evidence from Ps receiver functions
877 and thermobarometry of Neogene basalts (PICASSO project). Geochemistry,
878 Geophysics, Geosystems 15, 1113-1127.

879 Torne, M., 1996. Lithospheric structure of the Valencia trough. A brief review. In:
880 Tertiary basins of Spain, the stratigraphic record of crustal kinematics. Friend, P.F. and
881 Dabrio, C.J. (Eds). Cambridge University Press, E2, 49-54, 400 pp.

882 Torne, M., Fernàndez, M., Comas, M.C., Soto, J.I., 2000. Lithospheric structure beneath
883 the Alboran Basin: results from 3D gravity modeling and tectonic relevance. Journal of
884 Geophysical Research: Solid Earth 105, 3209-3228.

885 Torres-Roldán, R.L., Poli, G., Peccerillo, A., 1986. An Early Miocene arc-tholeiitic
886 magmatic dike event from the Alboran Sea - Evidence for precollisional subduction and
887 back-arc crustal extension in the westernmost Mediterranean. Geologische Rundschau
888 75, 219-234.

889 Turco, E., Macchiavelli, C., Mazzoli, S., Schettino, A., Pierantoni, P.P., 2012.
890 Kinematic evolution of Alpine Corsica in the framework of Mediterranean mountain
891 belts. Tectonophysics 579, 193-206.

892 Turner, S.P., Platt, J.P., George, R.M.M., Kelley, S.P., Pearson, D.G., Nowell, G.M.,
893 1999. Magmatism associated with orogenic collapse of the Betic–Alboran Domain, SE
894 Spain. Journal of Petrology 40, 1011-1036.

895 Van der Voo, R., 1993. Paleomagnetism of the Atlantic Thethys and Iapetus Oceans.
896 Cambridge University Press, Cambridge, United Kingdom, p. 411.

897 van Hinsbergen, D.J.J., Vissers, R.L.M., Spakman, W., 2014. Origin and consequences
898 of western Mediterranean subduction, roll-back, and slab segmentation. Tectonics 33,
899 393-419.

900 Vergés, J., Fernàndez, M., 2012. Tethys–Atlantic interaction along the Iberia–Africa
901 plate boundary: The Betic–Rif orogenic system. Tectonophysics 579, 144-172.

902 Vergés, J., Sàbat, F., 1999. Constraints on the Neogene Mediterranean kinematic
903 evolution along a 1000 km transect from Iberia to Africa. Geological Society, London,
904 Special Publications 156, 63-80.

905 Wilson, M., Bianchini, G., 1999. Tertiary-Quaternary magmatism within the
906 Mediterranean and surrounding regions. Geological Society Special Publication, 141-
907 168.

908 Wortel, R., Govers, R., Spakman, W., 2009. Continental collision and the STEP-wise
909 evolution of convergent plate boundaries: from structure to dynamics, in: Lallemand, S.,
910 Funiciello, F. (Eds.), Subduction Zone Geodynamics. Springer Berlin Heidelberg, 47-
911 59.

912 Zeck, H.P., Kristensen, A.B., Nakamura, E., 1999. Inherited Palaeozoic and Mesozoic
913 Rb–Sr isotopic signatures in Neogene calc-alkaline volcanics, Alborán Volcanic
914 Province, SE Spain. Journal of Petrology 40, 511-524.

915

Figure captions

Fig. 1. Sketch map of the Cenozoic orogenic (subduction related) and anorogenic (intraplate) volcanism in Europe, superimposed on the tectonic map of the region modified after Vergés and Sàbat (1999). From west to east: BB, Beni Bousera; R, Ronda; AS, Alboran Sea; MA, Murcia–Almeria; WA, Western Alps; S, Sisco; V, Veneto; SC, Sicily Channel; RP, Roman Province; C, Campania; AA, Aeolian Arc; E, Etna; IL, Insubric Line.

Fig. 2. Timing of anorogenic and orogenic volcanism from the Atlantic Ocean Islands, the Canaries and Madeira, and the Western and Central Mediterranean regions used in this paper for statistical purposes. For references refer to Fig. 4.

Fig. 3. Representative binary plots of the rotated component matrix in terms of F2 vs. F1 (**A**), F3 vs. F1 (**B**) and F5 vs. F3 (**C**) diagrams. See text for a comprehensive explanation.

Fig. 4. Orogenic and anorogenic volcanic rocks of Central (**A**, **C** and **E**) and Western (**B**, **D** and **F**) Mediterranean after the statistical analysis. See text for a comprehensive explanation.

Fig. 5: Representative binary diagrams of the factor scores of Central (**A**, **C** and **E**) and Western (**B**, **D** and **F**) Mediterranean volcanic rocks after the statistical analysis. Samples have been distinguished only on the basis of their age [using different colors following the Commission for the Geological Map of the World (http://www.ccgm.org)] and on the type of geodynamic environment they are linked to. F2 vs. F1 (**A, B**), F3 vs. F1 (**C, D**) and F5 vs. F3 (**E, F**) diagrams. Light blue and light red represent the anorogenic and lamproitic fields, respectively. “Slab dehydration”

939 indicates that the origin of the volcanic rocks is related to those processes responsible of
940 the dehydration of the subducting slab. When the features of the volcanic rocks need the
941 involvement of sediments in the metasomatic processes of the mantle wedge we used
942 the wording "increasing of sediment recycling". The dashed arrows indicate the
943 temporal evolution of the Tuscany trend (**A**) and of the samples from Spain (**B**).
944 Anorogenic volcanic data are from: Canary Islands, Madeira, Portugal, Spain,
945 Maghrebian Africa (Morocco), France, Italy (Sardinia, Ustica, Sicily Channel, Etna-
946 Hyblean and Veneto Province) and Germany (Lustrino and Wilson, 2007 and references
947 therein). Orogenic volcanic data are from: Western Alps, France (Corsica – Sisco),
948 Tuscany, Roman Province, Campania, Aeolian Islands, Betics, Alboran Sea, Morocco
949 (Gourougou and Guilliz), Sardinia (Lustrino et al., 2011 and references therein).

950 Fig. 6. Schematic tectonic maps showing the evolution of the Western Mediterranean
951 since 230 Ma (modified after Jiménez-Munt et al., 2010) Rheic oceanic suture, front of
952 the Variscan belt and major tectonic discontinuities are from Simancas et al. (2005).
953 Modifications of the mantle beneath the Western Mediterranean are probably linked to
954 episodes related to the collision which produced the Variscan Orogeny in the Middle
955 Triassic coupled to the depletion events due to partial melting triggered by subduction
956 of rifting phases (see text for details).

957 Fig. 7. Topographic map of the Central and Western Mediterranean with the distribution
958 of HP metamorphic complexes along the Betic–Rif system (Internal Betics and Internal
959 Rif), and along the Tellian fold belt in northern Africa (Great and Lesser Kabylies)
960 (modified after Vergés and Fernàndez, 2012). Light orange and orange arrows separated
961 by black dashed line indicate the NW and SE dipping subduction respectively (the
962 double polarity subduction model proposed by Vergés and Fernàndez, 2012). Dashed

963 white lines indicate other active or inactive faults separating the Alps from the
964 Apennines and the Kabylies. GB stands for Guadalquivir Bank**.**

Table captions

Table 1: Initial Eigenvalues, extraction and rotation of the sums of the squared loadings from factor analysis.

Table 2: Rotated component matrix of the calculated seven factors. Bold represents the best correlation between geochemical elements and factors.

Supplementary Material

Supplementary Table: Factor scores of the samples used for the statistical analysis.

Supplementary Figure. Binary diagrams resulting from the combination of all the calculated factors.

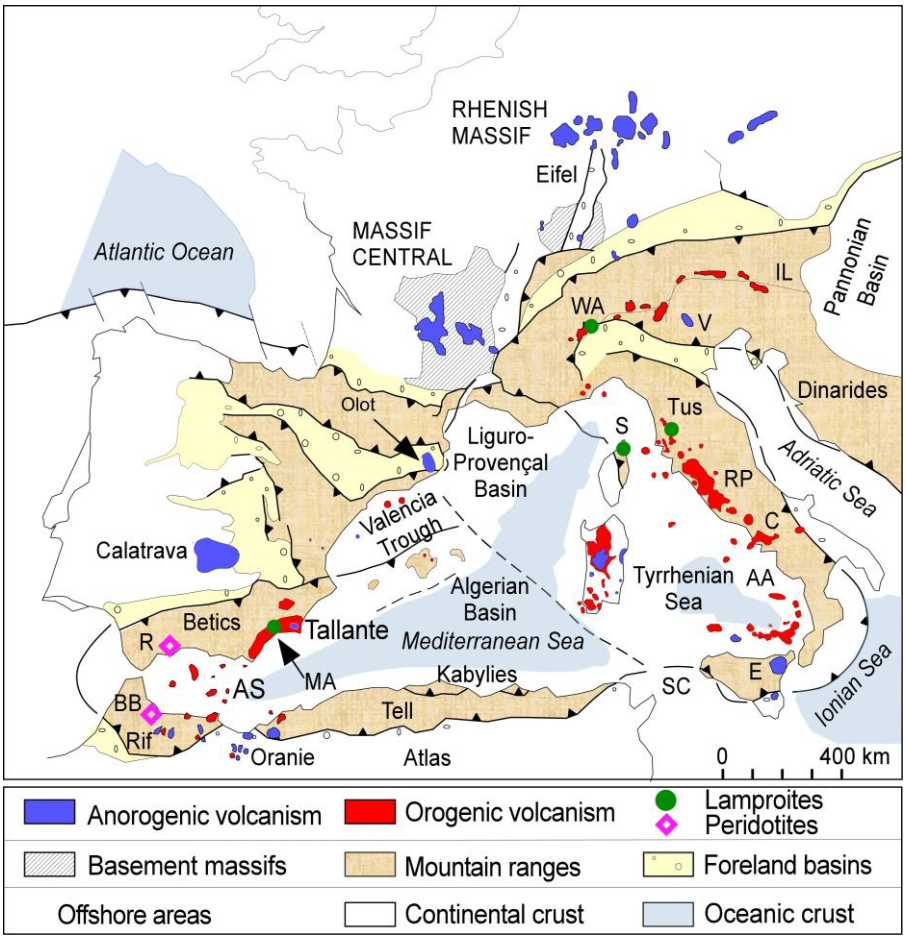

Fig. 1. Sketch map of the Cenozoic orogenic (subduction related) and anorogenic (intraplate) volcanism in Europe, superimposed on the tectonic map of the region modified after Vergés and Sàbat (1999). From west to east: BB, Beni Bousera; R, Ronda; AS, Alboran Sea; MA, Murcia–Almeria; WA, Western Alps; S, Sisco; V, Veneto; SC, Sicily Channel; RP, Roman Province; C, Campania; AA, Aeolian Arc; E, Etna; IL, Insubric Line.

977

978

979

980

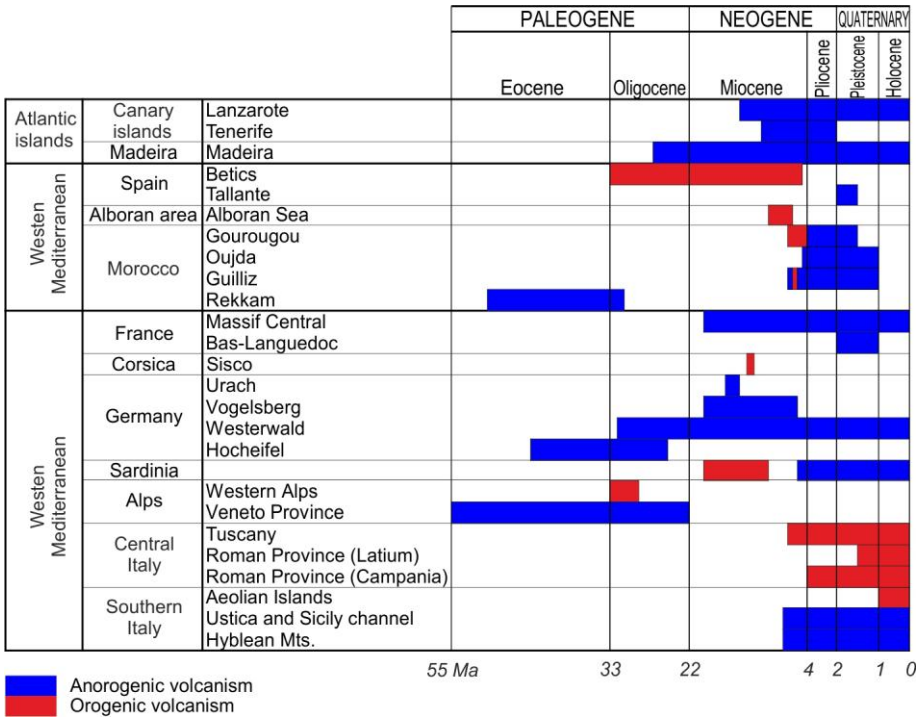

Fig. 2. Timing of anorogenic and orogenic volcanism from the Atlantic Ocean Islands, the Canaries and Madeira, and the Western and Central Mediterranean regions used in this paper for statistical purposes. For references refer to **Fig. 4**.

981

982

983

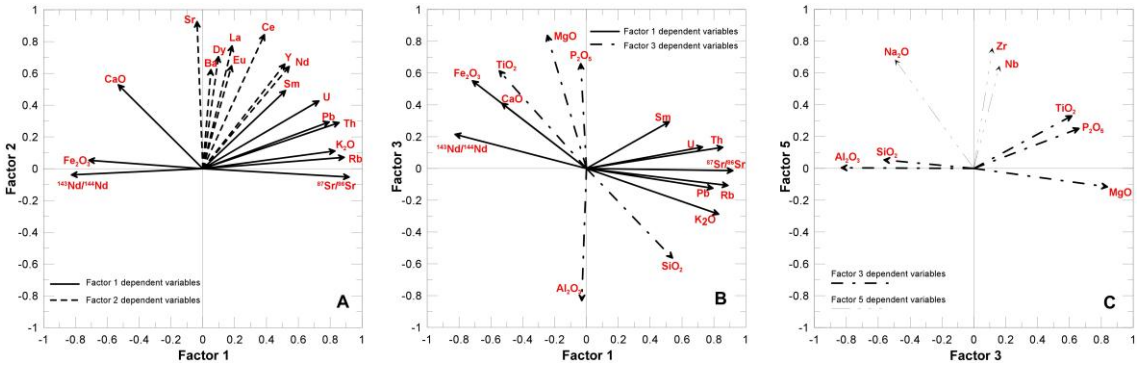

Fig. 3. Representative binary plots of the rotated component matrix in terms of F2 vs. F1 (**A**), F3 vs. F1 (**B**) and F5 vs. F3 (**C**) diagrams. See text for a comprehensive explanation.

984

985

986

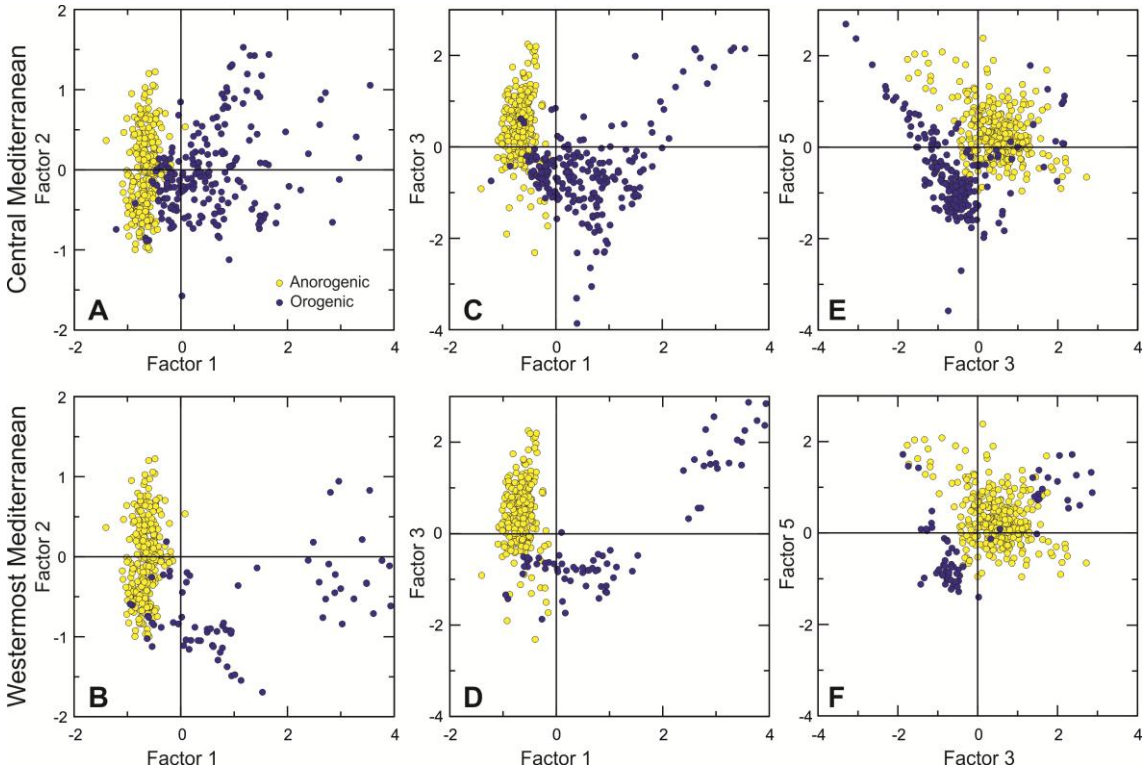

Fig. 4. Orogenic and anorogenic volcanic rocks of Central (**A**, **C** and **E**) and Western (**B**, **D** and **F**) Mediterranean after the statistical analysis. See text for a comprehensive explanation.

987

988

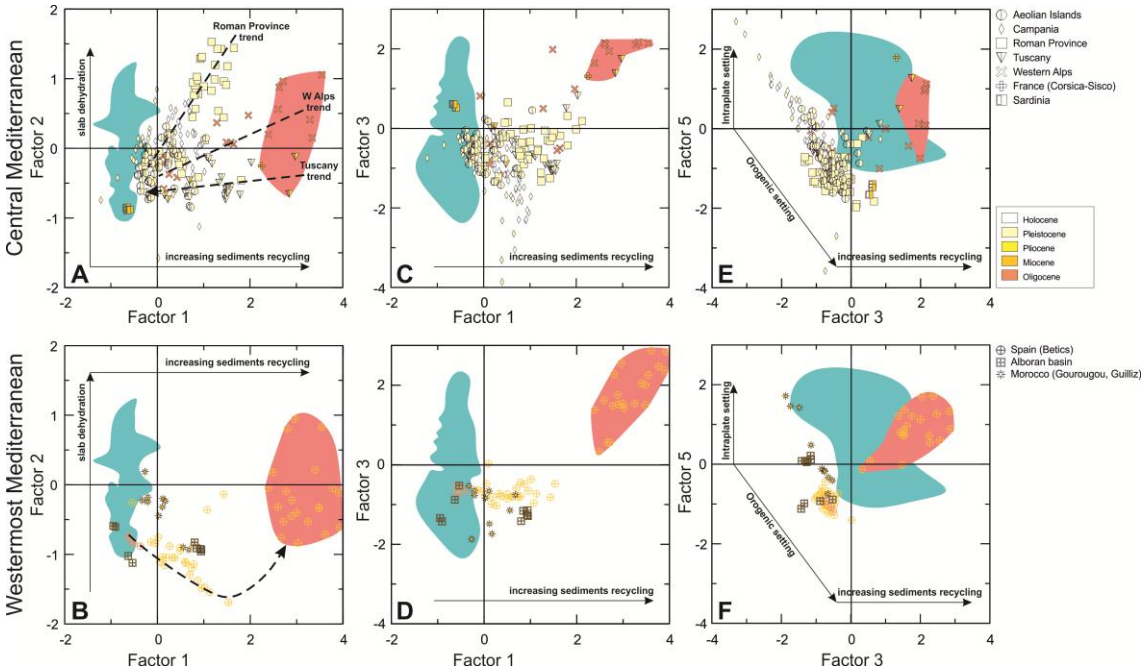

Fig. 5: Representative binary diagrams of the factor scores of Central (A, C and E) and Western (B, D and F) Mediterranean volcanic rocks after the statistical analysis. Samples have been distinguished only on the basis of their age [using different colors following the Commission for the Geological Map of the World (http://www.ccgm.org)] and on the type of geodynamic environment they are linked to. F2 vs. F1 (A, B), F3 vs. F1 (C, D) and F5 vs. F3 (E, F) diagrams. Light blue and light red represent the anorogenic and lamproitic fields, respectively. "Slab dehydration" indicates that the origin of the volcanic rocks is related to those processes responsible of the dehydration of the subducting slab. When the features of the volcanic rocks need the involvement of sediments in the metasomatic processes of the mantle wedge we used the wording "increasing of sediment recycling". The dashed arrows indicate the temporal evolution of the Tuscany trend (A) and of the samples from Spain (B). Anorogenic volcanic data are from: Canary Islands, Madeira, Portugal, Spain, Maghrebian Africa (Morocco), France, Italy (Sardinia, Ustica, Sicily Channel, Etna-Hyblean and Veneto Province) and Germany (Lustrino and Wilson, 2007 and references therein). Orogenic volcanic data are from: Western Alps, France (Corsica – Sisco), Tuscany, Roman Province, Campania, Aeolian Islands, Betics, Alboran Sea, Morocco (Gourougou and Guilliz), Sardinia (Lustrino et al., 2011 and references therein).

989

990

991

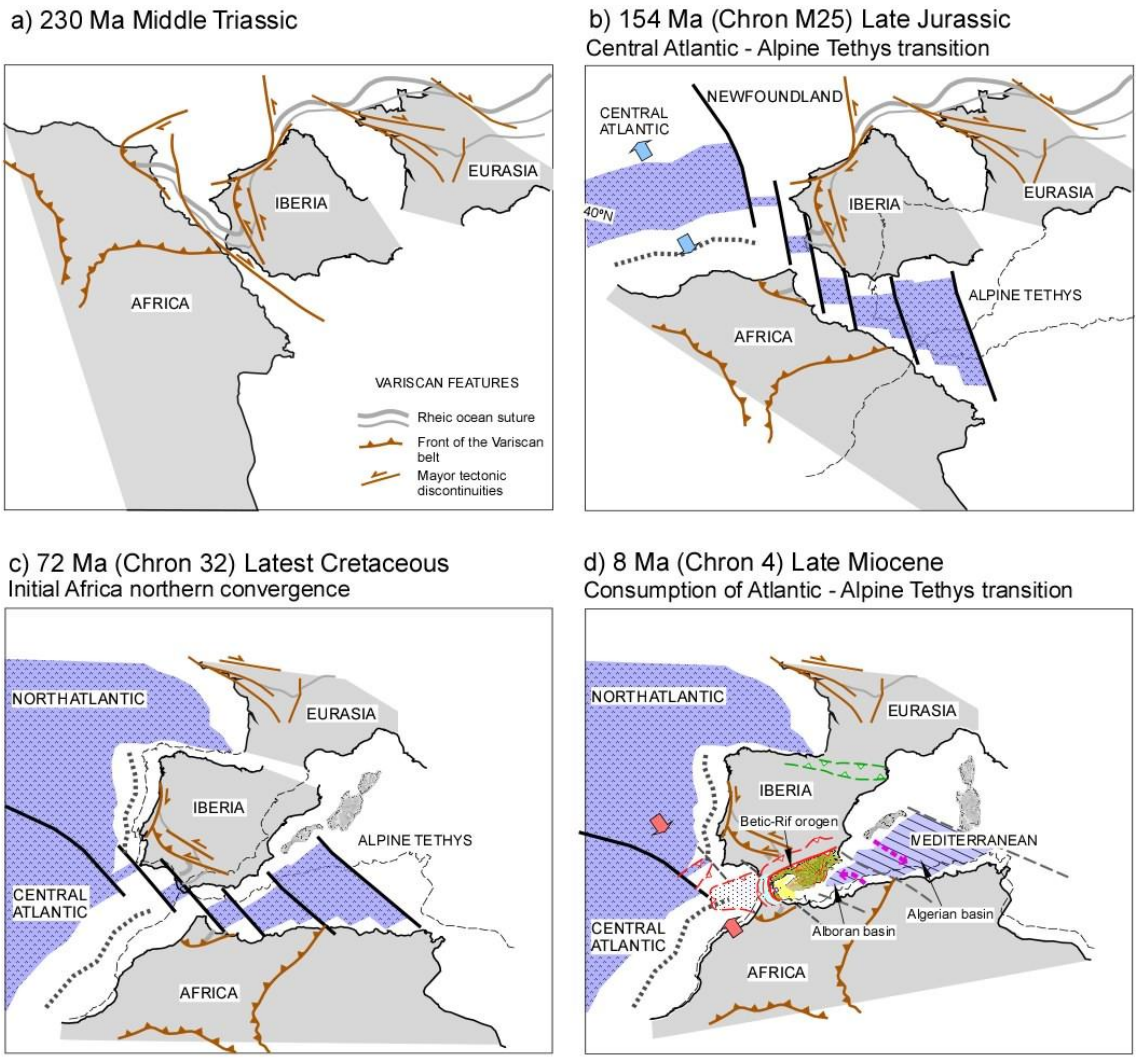

Fig. 6. Schematic tectonic maps showing the evolution of the Western Mediterranean since 230 Ma (modified after Jiménez-Munt et al., 2010) Rheic oceanic suture, front of the Variscan belt and major tectonic discontinuities are from Simancas et al. (2005). Modifications of the mantle beneath the Western Mediterranean are probably linked to episodes related to the collision which produced the Variscan Orogeny in the Middle Triassic coupled to the depletion events due to partial melting triggered by subduction of rifting phases (see text for details).

992

993

994

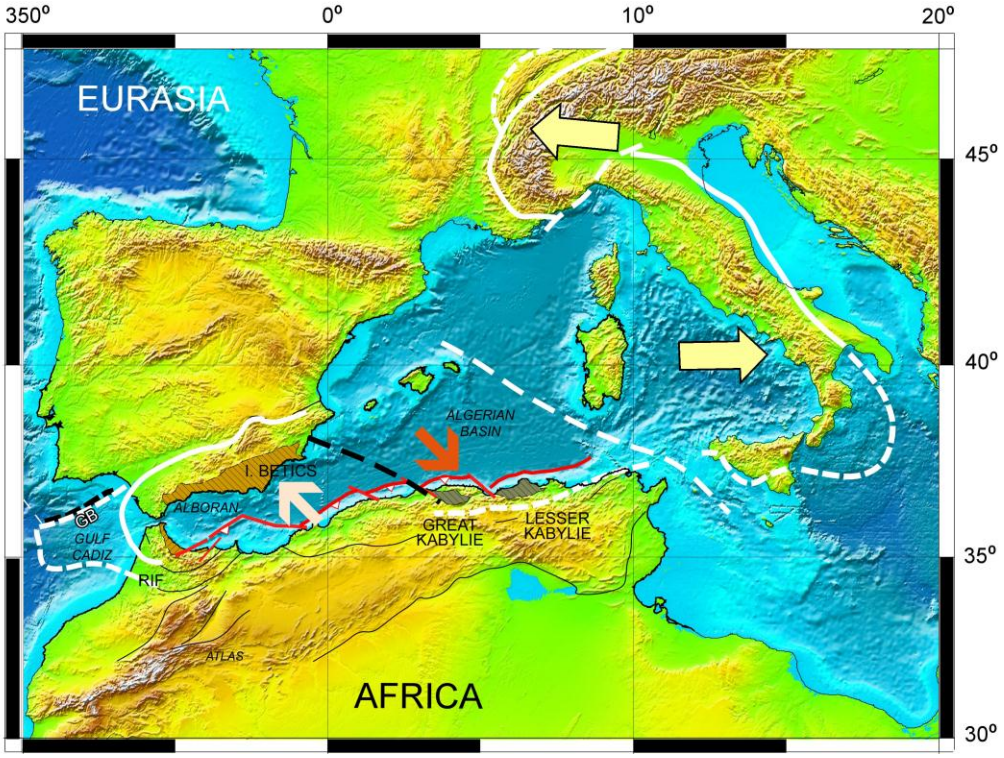

Fig. 7. Topographic map of the Central and Western Mediterranean with the distribution of HP metamorphic complexes along the Betic–Rif system (Internal Betics and Internal Rif), and along the Tellian fold belt in northern Africa (Great and Lesser Kabylies) (modified after Vergés and Fernàndez, 2012). Light orange and orange arrows separated by black dashed line indicate the NW and SE dipping subduction respectively (the double polarity subduction model proposed by Vergés and Fernàndez, 2012). Dashed white lines indicate other active or inactive faults separating the Alps from the Apennines and the Kabylies. GB stands for Guadalquivir Bank**.**

995

Table 1: Initial Eigenvalues, extraction and rotation of the sums of the squared loadings from factor analysis

	Initial Eigenvalues			Extraction Sums of Squared Loadings			Rotation Sums of Squared Loadings		
Component	Total	% of Variance	Cumulative %	Total	% of Variance	Cumulative %	Total	% of Variance	Cumulative %
1	11.318	31.438	31.438	11.318	31.438	31.438	8.183	22.732	22.732
2	7.595	21.098	52.536	7.595	21.098	52.536	6.697	18.602	41.333
3	3.990	11.084	63.620	3.990	11.084	63.620	4.410	12.249	53.582
4	2.447	6.796	70.416	2.447	6.796	70.416	4.234	11.762	65.344
5	2.125	5.902	76.318	2.125	5.902	76.318	2.302	6.394	71.738
6	1.565	4.347	80.665	1.565	4.347	80.665	2.270	6.306	78.044
7	1.265	3.513	84.178	1.265	3.513	84.178	2.208	6.134	84.178

Table 2: Rotated component matrix of the calculated seven factors. Bold represents the best correlation between geochemical elements and factors.

	Factors						
	1	2	3	4	5	6	7
SiO_2	.540	-.456	**-.563**	.023	.054	-.209	-.169
TiO_2	-.547	.037	**.614**	.068	.330	.132	.190
Al_2O_3	-.030	-.172	**-.831**	.018	.004	.182	-.004
Fe_2O_3	**-.715**	.053	.552	.056	-.033	.166	.142
MgO	-.246	.022	**.837**	-.115	-.115	.068	.050
CaO	**-.531**	.527	.410	-.013	-.406	.119	.077
Na_2O	-.346	-.019	-.494	-.031	**.683**	-.086	-.005
K_2O	**.829**	.111	-.287	.084	.134	.026	.096
P_2O_5	-.036	.510	**.659**	.113	.251	.083	.108
$^{87}Sr/^{86}Sr$	**.919**	-.053	-.014	.038	-.149	.095	-.123
$^{143}Nd/^{144}Nd$	**-.825**	-.039	.215	-.017	.285	-.074	.204
$^{206}Pb/^{204}Pb$	-.361	.082	.180	-.031	.138	-.162	**.828**
$^{208}Pb/^{204}Pb$	.020	.121	.037	-.004	.014	-.122	**.915**
$^{208}Pb/^{206}Pb$	.003	.042	.041	-.073	.000	**.974**	-.100
$^{207}Pb/^{206}Pb$	.016	.034	.030	-.070	-.006	**.969**	-.156
Rb	**.888**	.071	-.107	.128	.055	.028	.072
Sr	-.036	**.925**	.059	.065	-.136	.021	-.018
Ba	.515	**.658**	.170	.029	-.002	.055	-.136
Y	.051	**.623**	-.236	.406	.099	-.085	.296
Zr	.449	.231	.116	.041	**.757**	.081	.140
Nb	-.317	.526	.161	.053	**.644**	-.027	.135
La	.184	**.772**	.038	.408	.173	-.012	-.015
Ce	.387	**.843**	.083	.173	.158	-.002	.096
Pr	.394	.529	.204	**.625**	.016	.017	-.043
Nd	.543	**.643**	.233	.175	.151	.051	.103
Sm	**.519**	.491	.294	.345	.163	.069	.052
Eu	.180	**.647**	.443	.371	.232	.195	.105
Tb	.221	.205	.095	**.843**	-.026	.050	-.042
Dy	.098	**.705**	.026	.366	.185	.003	.353
Ho	-.059	.218	.028	**.885**	-.036	-.048	.053
Tm	.098	.091	-.097	**.933**	-.033	-.115	-.074
Yb	.112	.450	-.498	.334	.209	-.204	.358
Lu	.061	.236	-.402	**.666**	.246	-.106	.120
Th	**.855**	.290	.133	.148	.137	-.065	-.045
Pb	**.793**	.294	-.124	.122	-.029	.047	.018
U	**.729**	.426	.135	.156	.026	-.168	-.124